FACULTY OF SCIENCE
UNIVERSITY OF SOUTH BOHEMIA
ČESKÉ BUDĚJOVICE 2008

Master thesis

Effect of temperature on gill morphology and ion transporter distribution in the gills of Koi carp (*Cyprinus carpio* L.)

Hana Kratochvilová
Local supervisor: Pavel Blažka
External supervisors: James B. Claiborne
Susan L. Edwards

Master thesis

KRATOCHVILOVÁ H., 2008. Effect of temperature on gill morphology and ion transporter distribution in the gills of Koi carp (*Cyprinus carpio* L.). Mgr. Thesis, in English – 33 p., Faculty of Science, The University of South Bohemia, České Budějovice, Czech Republic.

Annotation

The effect of temperature on the gill morphology and ion transporter distribution in the branchial epithelium of a freshwater teleost, the Koi carp (*Cyprinus carpio*, L.) was examined. Three different water temperatures were used to detect changes in expression level of transporter proteins in the gill epithelial cells. With increasing temperature, the number of cells expressing the three ion transporters studied declined, and the gill lamellae protruded out of the cell mass, thus increasing the surface area of the branchial epithelium. A hypothetical organization of the transporter proteins within the ionocytes is proposed.

Prohlašuji, že svoji diplomovou práci jsem vypracovala samostatně pouze s použitím pramenů a literatury uvedených v seznamu citované literatury.

Prohlašuji, že v souladu s § 47b zákona č. 111/1998 Sb. v platném znění souhlasím se zveřejněním své diplomové práce, a to v nezkrácené podobě elektronickou cestou ve veřejně přístupné části databáze STAG provozované Jihočeskou univerzitou v Českých Budějovicích na jejích internetových stránkách.

8. ledna, 2008 …….

Hana Kratochvilová

ACKNOWLEDGEMENT

At the first place I want to thank the Dean and the whole Faculty of Science in České Budějovice because I could have never done this great and enjoyable work without their financial support. I also have to mention the Language Department, especially Rich Klee, who helped me fill in all the papers for the immigration office before leaving to USA.

Of course, this work could also have never been done without my American supervisors, JB Claiborne and Sue Edwards; they were like my adoptive family for all the seven months I spent with them. And Andrew Diamanduros was always the one to ask for help anytime.

My Czech supervisor, Pavel Blažka, and my colleague, Honza Okrouhlík, were those who made the final suggestions and corrections to this work. It was a great deal of unpleasant work and I truly appreciate their effort.

Not only did the financial support come from the school, but from my family as well, especially my grandfather. I promise to try to be at least as good granddaughter, daughter, and sister as I have been so far.

My friends prepared a supportive atmosphere for me during all the school years. Thank ya'll!

Contents

Introduction

Koi carps

The name koi comes originally from a Japanese word nishikigoi, meaning "Japanese colored carp". Koi is derived from the wild common carp (*Cyprinus carpio*, L.), family Cyprinidae. However, according to Balon (1995), koi did not derive directly from the wild carp, but rather from feral or domesticated pond forms.

Common carp is a eurythermal freshwater species, which originated in western central Asia, and spread to the East to Siberia and China, and to the West to Europe. From here, it continued then all over the temperate world of the northern hemisphere with the monks who bred this fish at the monasteries (Axelrod et al., 1996).

Typically, adult common carp has a body length from 25 to 75cm, but exceptionally up to 1.5m. The maximal recorded weight was 35kg. The life span can reach over 40 years. There are 13 other types of carp of the genus *Cyprinus* (Hanel, 1998, Reichholf and Steinbach, 2002).

Red or golden morphs are quite frequent among cyprinid species, particularly in Crucian and Prussian carp (*Carassius c.*, *C. gibelio* – gibel), tench (*Tinca t.*), and ide (*Leuciscus idus*). Koi appeared first in Echigo, Niigata prefecture, Japan, about 100 years ago from color aberrant phenotypes of wild carp, although some authors suggest that koi could have been introduced to Japan from China (Wang and Li, 2004). Currently, there are 15 different color types, each one with several other sub-forms (Hanel, 1998). They became very popular within Japan in the first half of the twentieth century. Later that century, with their increasing popularity, they were brought also to other parts of the world, such as Israel or the United States. The first koi were imported to Florida in about 1960 (Axelrod et al., 1996).

Gills

The first primordial fishes' interior milieu was isosmotic to the ambient environment, the seawater. With the evolution of more complex forms and their adaptation to different environments, the need to compensate for external changes became more urgent. Therefore, more advanced fishes developed different organs (kidneys, skin,

gills, etc.) to maintain the internal homeostasis (Moyes and Schulte, 2006). In teleost fish, the gills serve not only as a site of gas exchange, but it is also the main ion and acid-base balancing organ (over 90% of acid-base compensatory activity – Evans et al., 2005).

Anatomy

The teleost branchial apparatus consists of four gill arches on either side of the head covered with an operculum as shown in Figure 1 (Graham, 2006). The gill epithelium, covered with a protective mucous layer, is formed of the gill filaments – two rows on each arch. Each filament has a lower and an upper row of lamellae. This whole arrangement forms a sieve-like structure with large surface area that allows the gill to maximize the efficiency in gas and ion transfer (Fig. 2) (Randall et al., 2002).

The inner lamellar wall is composed of pillar cells that form tube-like spaces (lacunas) for blood circulating in a countercurrent to water pumped through the gills. When passing through the lacuna, the red blood cells slow down and squeeze, thus probably enhancing the gas exchange (Stensløkken et al., 1999).

The branchial epithelium consists of several cell types, such as mucus and neuro-epithelial cells (Perry, 1997). The two types most important for osmoregulation are the pavement cells (PVCs) and the mitochondria rich cells (MRCs – also called chloride cells). A substantial fraction of the branchial epithelium is covered with PVCs, which are usually believed to play role in gas exchange. However, according to some experiments (Hwang and Lee, 2007, Perry, 1997, Sullivan et al., 1995, Wilson et al., 2000) the PVCs, at least in freshwater species, might also be active in osmoregulation. Some results suggest that the PVCs containing a higher amount of mitochondria might actually be a sub-type of MRCs, or at least two types of MRCs are found in the branchial epithelium (Chang et al., 2000, Choe et al., 2004, Galvez et al., 2001, Hwang and Lee, 2007, Perry and Gilmour, 2006).

MRCs are thicker than the PVCs (Randall et al., 2002), but they represent a smaller portion (less than 15%) of epithelial cells exposed to the environment (Evans et al., 2005, Hwang and Lee, 2007, Perry, 1997). They occur mostly on the afferent (trailing)

edge in the interlamellar region, but under certain conditions they can be found also on the lamellae where they may inhibit the transfer of respiratory gases (Perry, 1997). As mentioned above, there are at least two types of MRCs, differing in ultrastructure, mitochondria density, autofluorescence, and peanut lectin agglutinin (PNA) binding (Choe et al., 2004, Galvez et al., 2002, Moyes and Schulte, 2006). However, according to Galvez et al. (2002), differences in ultrastructural and autofluorescence properties do not provide any evidence to consider these sub-types as functionally different. On the other hand the authors claim that the differences in PNA binding (PNA^+) and PNA not binding (PNA^-) cells suggest also to the differences in function whereas the PNA^+ cells show some functional similarities to the base secreting β-MR cells (Pisam et al., 2000). In the PNA^- cells fraction, Galvez et al. (2002) found cells with high amounts of mitochondria with morphological features more similar to pavement cells. These cells are suggested to be the site of H^+ excretion in the freshwater branchial epithelium.

Regulation in seawater

MRCs are the main osmoregulatory cells in seawater teleost gills (Fig. 3.). Marine fish take up ions passively, whereas they lose water to the environment. For rehydration, they ingest water and maintain osmoregulatory homeostasis by excreting the excess salts (mainly NaCl) via the MRCs. Basolateral Na^+/K^+ ATPase (NKA) produces an electrochemical sodium gradient, which facilitates Cl^- entry via $Na^+/K^+/2Cl$ co-transporter (NKCC). Cl^- accumulates intracellularly above the electrochemical equilibrium and exits the cell passively via an apical anion channel (CFTR – cystic fibrosis transmembrane conductance regulator). The first CFTR was cloned from seawater-adapted killifish (*Fundulus heteroclitus*) by Singer et al. (1998). This produces a negative charge on the outer side of the apical membrane, which is believed to enable the passive secretion of Na^+ ions down the electrochemical gradient through a cation-selective pathway between MR and accessory cells (Daborn et al., 2001, Marshall and Grosell, 2006). Apical Na^+/H^+ exchanger (NHE) is proposed to secrete protons to the external environment. This efflux is balanced by passive influx

of sodium ions down the concentration gradient, i.e. without energetic demands (Claiborne et al., 2002).

Regulation in freshwater

Freshwater (FW) regulation is more ambiguous. The internal plasma of FW fish is hyperosmotic compared to the external water. Therefore, the fish tend to lose ions by diffusion or by renal excretion to the environment, and have to counteract this loss by absorbing the ions back through the branchial epithelium (Moyes and Schulte, 2006).

There are several models explaining the possible mechanisms of the ion uptake through the branchial epithelia in freshwater fish. These models often involve MRCs, which have high metabolic activity and are characteristic for the expression of basolarteral Na^+/K^+ ATPase (NKA). This enzyme maintains a low intracellular Na^+ concentration and provides a gradient for Na^+ entry into the cell from water. There are two suggested ways for the Na^+ uptake. Previously, the model involved a Na^+/H^+ exchanger (NHE), which absorbed the external Na^+ into the cell for the exchange of protons that were generated by H_2CO_3 dissociation via carbon anhydrase II (CA II) (Evans et al., 2005, Hirata et al., 2003). The role of NHE in FW Na^+ uptake has been questioned because the gradient for NaCl uptake into the cell is unfavorable and would require some driving force in the form of ATP (e.g. Wilson et al., 2000).

Some of the studies from the last 15 years propose a different model for the FW sodium uptake. It involves apical vacuolar H^+ ATPase (V-HAT) that generates a favorable electrical gradient by excreting protons out of the cell to the water. This gradient enables the sodium ions to be taken up through the epithelial Na^+ channel (ENaC) (Avella and Bornancin, 1989, Katoh et al., 2002, Lin et al., 1994, Perry 1997, Wilson et al., 2000). Since V-HAT is found in the apical membrane and excretes protons directly to the external environment, it could also contribute to the acid-base balance (Claiborne et al., 2002, Perry and Gilmour, 2006). However, it is still not clear, in which cells (PVCs or MRCs) this transporter occurs. It was found in both types in the rainbow trout *Oncorhynchus mykiss* (Lin et al., 1994), but only in PVCs and not in MRCs of tilapia *Oreochromis mossambicus* (Wilson et al., 2000). In low-NaCl environment acclimated killifish *Fundulus heteroclitus*, V-HAT was even found

in the basolateral membrane of MRCs (Katoh et al., 2002). These conflicting results suggest that there are likely variations between species.

As already mentioned, sodium can exit the epithelial cell via a basolateral NKA. According to some recent studies, such as Hwang and Lee (2007), also a different transporter may be involved in this transfer, namely a Na^+/HCO_3^- co-transporter (NBC). This organization can also be found in the proximal tubule of the mammalian kidneys (Amlal et al., 2001).

Ion transporters

Na^+/K^+ ATPase (NKA)

This enzyme may be found in membranes of virtually all animal cells. The main function of NKA is to maintain a certain membrane potential by keeping the intracellular concentration of sodium 10-20 times lower than the extracellular, and opposite for the potassium. It binds Na^+ and ATP on the intracellular and K^+ on the external surface, and exports three sodium ions in exchange for importing two K^+. The membrane potential provides then a driving force for the transmembrane movement of other substances. The constant pumping of the ions through this enzyme consumes a lot of energy in the form of ATP (as much as 25%, Randall et al., 2002), and in anoxia, this transporter can account for up to 75% of the ATP demands of the cell (Hochachka and Lutz, 2001). It is composed of an α-subunit, which spans the membrane ten times and a β-subunit spanning the membrane only once (Blanco and Mercer, 1998, Fig. 4.). In the fish gill, it is found mostly on the basolateral membrane of the MRCs and is believed to transport sodium ions out of the cell into the plasma. Recently however, the role of NKA in FW sodium basolateral transport has been questioned (see Discussion).

V-H^+-ATPase (V-HAT)

V-HAT functions in almost every eukaryotic cell as an ATP-dependent proton pump. It was first located in organelles linked to the vacuolar system and is responsible for the acidification of the intracellular compartments (pH as low as 0.1 in vacuoles of brown and red algae). The proton-motive force, generated by this enzyme, also

energizes other secondary transport processes, e.g. particularly in the apical plasma membranes of epithelial cells. It is composed of a catalytic part, V_1, and a non-catalytic membrane sector, V_0. The V_1 part consists of a catalytic unit, a shaft and a hook, and the membrane part represents a proton turbine (Nelson and Harvey, 1999, see also Fig. 5.). As reviewed in Evans et al. (2005), freshwater vertebrates utilize V-HAT as a driving force for NaCl uptake; V-HAT, located in the apical membrane of MRCs, generates a gradient that drives sodium entry via an apical Na^+ channel (ENaC). Since protons are excreted to the external environment, this enzyme is suggested to be involved also in the fish acid-base regulation (Claiborne et al., 2002, Perry and Gilmour, 2006).

Na^+/H^+ exchangers (NHEs)

NHEs are integral plasma membrane proteins that exchange one extracellular sodium ion for one intracellular proton. They maintain the intracellular homeostasis, control the cell volume, and contribute to NaCl absorption in epithelia. At least ten members of the mammalian NHE family have been reported to date (Yan et al., 2007, in press). They differ in their tissue distribution, but all isoforms are suggested to have a similar membrane topology with a cytoplasmic region at the C terminus and 10-12 membrane helixes at the N terminus (Orlowski and Grinstein, 1997, see also Fig. 6.). In our study, we used antibodies against the type 3 of the NHE family. In mammals, NHE3 is mainly expressed in the apical membrane of the epithelial cells of the renal proximal tubule where it drives bicarbonate reabsorption (Amlal et al., 2001). In marine teleosts, it is also expressed apically and contributes to the acid excretion in exchange for passively entering sodium ions from the hyperosmotic environment (Claiborne et al., 2002). Formerly, the apical NHE was believed to contribute to Na^+ uptake also in FW fish. It has been questioned for a long time because there was no confirmed driving force that would overcome the unfavorable gradient. Some recent studies show however that there might be a combination of other transporters able to energize this ion uptake. Protons for this exchange may be provided by the H_2CO_3 dissociation. Sodium ions would then be secreted to the plasma via a basolateral Na^+/HCO_3^- cotransporter (NBC) (for details see Hwang and Lee, 2007).

Temperature – oxygen concentration relationship

Generally, water as a living medium is known for having a very low content of dissolved oxygen compared to air. Moreover, solubility of oxygen in water decreases with increasing temperature. According to experiments conducted by Dobihal and Blazka (1974 – concluding report of a project), the safe level of dissolved oxygen for swimming fish at 22°C equals 100% saturation of air in water; this point is at about 6.3 ml O_2/l. The safe level of dissolved oxygen is a level, at which there is still enough oxygen to supply all metabolic processes in the animal including sustainable swimming. It increases with water temperature, whereas the level of 100% saturation decreases, suggesting that the fish cope with moderate hypoxia at higher temperature (Fig.7.)

Alteration in the gill morphology

Some Cyprinid fishes (Crucian carp *Carassius carassius*, goldfish *C. auratus*, and Prussian carp *C. a. gibelio*) are known for their ability to survive long periods of hypoxia or even anoxia (Blazka, 1958, Kratochvilova, 2005 - Bachelor thesis). In addition, Crucian carp and goldfish appear to alter the morphology of their gills in differing environmental conditions. The lamellae of fish in normoxic conditions are embedded in a cell mass. Within seven days after the onset of hypoxia at 8°C, the gill lamellae of the Crucian carp protrude on the surface, increasing the surface area by ~7.5-fold (Sollid et al., 2003, Fig. 8.), and the gill arches then show the "typical" morphology as observed in most fishes. Similar results were described in animals exposed to high temperatures. When adapted to 15 and finally to 7.5°C at normoxic conditions (from 25°C in control fish), goldfish gradually covered the protruded lamellae with the cell mass (Sollid et al., 2005). The advantage of having lamellae embedded in the cell mass is to decrease the surface area through which the ions can be lost to water, and thereby to lower the energy costs for the uptake of these ions.

Objectives and hypotheses

Study the effect of temperature acclimation on gill morphology and transporter expression in the koi carp.

Suggest a putative model of ion regulatory mechanisms in freshwater fish branchial ionocytes.

Master the gill tissue processing and some of the immunohistochemical staining techniques.

The changing temperature may result in alteration of gill morphology in koi; since these fish have been bred more for their aesthetic qualities than for their ability to survive hypoxia, this change may be less obvious than that observed in Crucian carp.

Little is known about the variations in ion transporter expression in the osmoregulatory cells during temperature driven gill morphological changes. It is tempting to suggest that with the changing temperature and gill morphology, the expression level of the three ion transporters studied (NKA, V-HAT, and NHE3) will also vary in order to maintain homeostasis.

Materials and Methods

Animals

Koi carp were obtained from a retail pet store (Statesboro, GA, USA). Animals were housed in glass aquaria in aerated local tap freshwater until use. They were acclimated to three different experimental temperatures (4°C – cold, 22°C – control, and 28°C – hot) for a period of two weeks (n=3 for each experiment). Fish encounter 4°C when wintering in natural water pools, 22°C is close to the optimal temperature of this species (Metz et al. 2003), and 28°C is suggested to be close to the highest tolerable temperature.

Antibodies

Antibody α5 was developed by Dr. Douglas Fambrough, and was obtained from the Developmental Studies Hybridoma Bank at the University of Iowa, IA, USA. It was raised against the avian Na^+/K^+ ATPase α subunit and binds to all isoforms. This antibody recognizes fish NKA, and is now widely used for studies on fish branchial cells (e.g. Choe et al., 2004).

Dace Na^+/H^+ exchanger (dNHE3) antibody was provided by Prof S. Hirose, Tokyo Institute of Technology. Fragments of dNHE3 cDNA were isolated from the Osorezan dace (*Tribolodon hakonensis*) by RT-PCR with gill mRNA. The antibody was raised in rabbits in response to injection with dNHE3 – a 20-residue COOH-terminal synthetic peptide linked to keyhole limpet hemocyanin: DASVDEEASEEKPGKNHTRL.

The rabbit polyclonal antibody for vacuolar H^+-ATPase (V-HAT) was developed by ProSci Incorporated against a sculpin-HATB-A324 epitope: C-AREEVPGRRGFPGY, based on a partial sequence for V-HAT in sculpin (*Myoxocephalus octodecimspinosus*), GENEBANK: DQ520199.

Alexa Fluor 488 and Alexa Fluor 568 (Molecular Probes, Invitrogen, USA) are fluorescent dyes and were used as secondary antibodies. Alexa Fluor 488 (goat anti mouse) was used for staining of the NKA antibody, and the final product color was green. Alexa Fluor 568 (goat anti rabbit) was used for staining either V-HAT or NHE3 antibody, and the resulting color was red.

Immunofluorescence microscopy

Animals were terminally anaesthetized with MS 222 (0.01%; 3-aminobenzoic-acid-ethylesther methanesulfonate salt, Sigma, U.S.A.) followed by removal of the gill arches, which were placed into chilled 4% paraformaldehyde in 10 $mmol \cdot l^{-1}$ phosphate buffered saline (PBS) pH 7.4 for 4 hours, before transfer to PBS to remove the fixative. After washing, gill tissues were dehydrated in an increasing ethanol series, and cleared in CitriSolv (Fisher). CitriSolv replaces more toxic xylene. After washing in CitriSolv, the tissue was embedded in paraffin wax. Sections were cut at 5 μm thick parallel sections, and dried onto superfrost plus slides. These were then dewaxed through CitriSolv bath and rehydrated through a decreasing ethanol series followed by washing in PBS. The tissue on the slides was circled with a hydrophobic barrier (ImmEdge pen, Vector Laboratories, USA), blocked in 5% normal goat serum (NGS) in PBS for 30 min and incubated overnight with primary antibodies (diluted by 5% NGS with 3% triton 1:500 for NKA and dNHE3, 1:750 for HAT, respectively) in a humid chamber at room temperature. The next day, the tissue sections were washed in PBS, and incubated with secondary antibodies Alexa Flour 488 (for NKA) or Alexa Flour 568 (for NHE3 and HAT), both diluted 1:250 in PBS, for 1h at room temperature. The incubation was followed by washing in PBS, and mounting with antifade reagent, Prolong® Gold (Invitrogen, USA), which increases the stability of fluorescent staining. The sections were then covered with cover slips and viewed on an Axiovert fluorescence microscope, which was also used for counting of the immunopositive cells. Some images were also recorded on a Zeiss confocal microscope at the Mount Desert Island Biological Laboratory in Salisbury Cove, ME, USA. We used sections treated with normal goat serum and secondary antibody to account for non-specific background labeling as a negative control. A simplified scheme of the immunohistochemical staining is shown in Figure 9.

Counting

Positively stained cells for NKA, dNHE3, and V-HAT were counted for each fish on three different sections from two randomly selected filaments over 0.5 mm, thus

giving six values for each fish. Due to damaged gill tissue of one fish at 4°C, we had cell counts for only two fish from this group, but three fish from both the 22°C and 28°C group.

Measurement of surface area

The pictures made on the Axiovert fluorescence microscope were used to determine how much of the interlamellar space is covered with the cell mass. With the help of the Scion Image program (Scion Corporation, 2000), the area of the whole interlamellar space was measured first, followed by the measurement of the area covered with the cell mass. Percentage of the covered area was counted, and these data were processed statistically (see below). All the measurements were done on sections stained for NKA and NHE3. The covered surface area was measured over ten interlamellar spaces in a row within one picture, whereas the interlamellar areas with damaged or curved tissue were omitted. Since there were only two fish in the 4°C group, a random picture (with staining for the same protein) of one of these fish was chosen to measure other ten interlamellar spaces, giving 30 values for each temperature group.

Statistical analysis

Positively stained cell counts from each temperature group were compared against counts from both other groups separately for each ion transporter. Similarly, the percentage values of interlamellar cell mass of the temperature groups (30 data each) were compared against the two other groups.

Data were analyzed with the non-parametric Mann-Whitney U test using Statistica 7.1 (StatSoft, Inc., 2005). Significance was accepted at $P<0.05$. All values are expressed as means ± standard error of the mean (S.E.M).

Results

Immunohistochemistry

The gill sections were stained for NKA and dNHE3 or NKA and V-HAT, respectively, to determine whether the transporters co-localize in the same cells. We observed that the vast majority of positive cells seemed to express either one or the other and were not co-localized in the same cells. Moreover, probably due to a small size of the cells, the staining of all antibodies seemed to be spread throughout the cell body with the exception of the nucleus (Fig. 10.). Therefore, it was not possible to localize the transporters to either apical or basolateral membrane.

Changes in expression

The influence of three different water temperatures (cold – 4°C, control – 22°C, and hot – 28°C) on the number of cells expressing the three different ion transporters (NKA, V-HAT, dNHE3) was compared. Table 1 shows that the lowest expression count of NKA cells was seen in the hot group with a 23 fold increase to the control group and 34 fold increase to the cold group ($P<0.05$). Cells stained for dNHE3 were most abundant in the control group (53.89 ± 5.59 versus 26.58 ± 4.82 in cold group) with a six fold decrease to the hot group ($P<0.05$). The difference in expression of V-HAT in the cold (36.5) and control group (31.67) was not statistically significant ($p = 0.37$). However, there was an obvious decrease in number of V-HAT immunologically positive cells between the control and hot group ($P<0.05$). (Fig. 11. – 14.).

	NKA	**dNHE3**	**V-HAT**
4°C	30.58 ± 2.97	26.58 ± 4.82	36.50 ± 3.06*
22°C	20.61 ± 2.10	53.89 ± 5.59	31.67 ± 2.42*
28°C	0.89 ± 0.24	8.28 ± 1.48	18.00 ± 2.90

Tab.1. Counts of positively stained cells for three ion transporters at three temperatures over a surface area unit. Values are mean ratios ± s.e.m. (N=18 for control and hot group, and 12 for cold group). All values in one group are significantly different from each other ($p = 0.05$), except of the values marked with an asterisk ($p = 0.37$).

Surface area

The acclimation of the fish to different temperatures resulted in changes in gill morphology. Figure 15. shows that the lamellae in fish kept at 4°C were almost fully covered with the cell mass, ranging from 68 to nearly 100%. On the contrary, fish acclimated to the highest temperature increased the branchial surface area by lowering the cell mass down to 40% of the interlamellar space. The cell mass of the most of the control fish typically covered 72 to 83% of the space (Fig. 16.).

Discussion

Three different acclimation temperatures were used to examine the effect of temperature on ion transporter expression level and gill morphology in the freshwater koi. According to van den Thillart and van Waarde (1985) and Zhou et al. (2000), common carp have the ability to cope with hypoxic conditions. The first strategy of fish in moderate hypoxia is to maintain the oxygen delivery by increased gill ventilation and capacity of respiratory surfaces (Randall, 1982).

In our study we observed alteration of the gill morphology, as described for Crucian carp by Sollid et al. (2003) and Sollid et al. (2005). They examined the effect of both the temperature and decreased oxygen level and they concluded that the fish studied lowered the surface area when in normoxic conditions or at low temperature, respectively. The authors hypothesized that it was advantageous for the animal to have lamellae embedded in the cell mass to decrease the surface area through which ions can be lost to water, and thereby to lower the energy cost of the regulation of these ions. Clearly, a larger gill surface area allows for greater gas exchange through the epithelial surface, but these species (Crucian carp and goldfish) have a high capacity to take up enough oxygen in normoxic water even with covered lamellae (in part due to a high hemoglobin oxygen afinity; Sollid et al., 2003), and require higher exchange surface area only when in an environment with low O_2 concentration.

As discussed in the Introduction (Temperature – oxygen concentration relationship), at temperatures higher than 22°C, aquatic animals already cope with moderate hypoxia because the solubility of oxygen is not sufficient at this temperature (Fig. 7.). Moreover, ectotherms increase their metabolic rate (O_2 consumption) with increasing temperature (Randall et al., 2002). Thus, it can be concluded that the alteration in the gill morphology observed in our study could have been caused either by increased temperature (i.e. increased oxygen conspumption) or decreasing oxygen concentration (particularly at 28°C), or by a combination of these two factors.

The question emerging from these observations is**:** are fish with covered gill lamellae capable of sufficient ion uptake? Our results show more cells expressing the

ion transporters per surface area unit in covered lamellae (cold temperature) than in protruded; all three proteins (NKA, NHE3, and V-HAT) had the least cells expressing the transporters in the highest temperature. This corresponds to a research conducted by Metz et al. (2003); common carp were acclimated to 15, 22 or 29°C for eight weeks. The authors described differences in plasma osmolality, sodium, potassium and chloride concentrations between the groups studied following the acclimation, whereas plasma total and ionic calcium levels did not change, suggesting successful adaptation of the fish. They measured the NKA activity and explained their observations by its alteration. They also used immunohistochemical techniques to determine the expression level of NKA. This research implied that at lower temperature (15°C), the sodium pump's activity was decreased compared to higher temperatures, and as a compensatory mechanism, the fish increased the transporter's expression. On contrary, the higher ambient temperature (29°C) activated the enzyme; therefore, a lower expression level was sufficient.

V-HAT showed the smallest differences in the number of positive cells between the three temperature groups. This observation corresponds to a study on a low-pH-tolerating teleost, the Osorezan dace *Tribolodon hakonensis* (Hirata et al., 2003). Although this enzyme is believed to be one of the major acid-base balancing transporters, the authors did not find significant changes in the message or protein levels following the acidosis. They suggested that it probably does not play a central role in the acid adaptation. The effect of temperature on this enzyme is however not clear. Since we may expect that there were no or small changes in pH between the cold and control group, it is not surprising that the expression level of V-HAT did not change. For a better understanding of processes occurring in the hot group, we need more information on the activity level of the transporters.

Our results show a decrease in positively stained cells of both of the acid secreting transporters, NHE3 and V-HAT, in the hot group. If we hypothesize that the lower cell count occurs in paralell with a higher activity of the transporters (as observed in the

case of NKA by Metz et al., 2003), it is likely that the fish from the hot group experienced some form of acid load.

This acid load could have been caused by an increased activity of the fish: i) due to higher ventilation frequency – as discussed earlier, a mild hypoxia is likely to occur at 28°C; animals coping with a decreased oxygen level increase the ventilation frequency in order to gain enough oxygen (Randall, 1982); ii) due to motility of fish trying to find water with lower temperature. According to Randall et al. (2004), hypoxia adapted fish when exposed to an environment with a lower oxygen level tend to move to colder water which helps them to reduce energy expenditure. Saving energy is a typical physiological adaptation of hypoxia-tolerant animals, unlike the hypoxia non-adapted ones, which increase their nutrient consumption in glycolysis (Pasteur Effect).

A hypothetical FW model of the ion transporter organization is proposed in Figure 17. As expected, we did not detect any co-localization of NKA and V-HAT in the positively stained cells. This confirms observation of other authors (Hwang and Lee, 2007 and Piermarini and Evans, 2001). According to them, the apical V-HAT generates the driving force for Na^+ uptake which is then basolaterally secreted through a Na^+/HCO_3^- co-transporter (NBC). HCO_3^- for this transfer is produced from the metabolic CO_2, production is accelerated by carbon anhydrase (CA). This organization corresponds to H^+-ATPase-rich cells (HR) described by Hwang and Lee (2007).

The sodium uptake was proposed to occur via an apical Na^+ channel (ENaC). Perry and Gilmour (2006) pointed out that the genes of this transporter were so far not cloned. Recently however, Parks et al. (2007) suggested that the ENaC was present based on its phenamil-sensitivity, and proposed a model of sodium uptake through this transporter connected to V-HAT in the PNA^- MR cell fraction which represents 77% of all MRCs.

Although we cannot completely rule out the existence of some cells expressing both NHE3 and NKA, our observations suggest that these two transporters are expressed mostly in two different cell populations (Fig. 13). A possible explanation is that there might be a different NHE type, such as NHE2, expressed in the NKA

immunopositive cells. Scott et al. (2005) found that the killifish *Fundulus heteroclitus* decreased NHE3 expression after transfer to freshwater, whereas the expression of NHE2 type increased 1.7 fold. An alternative way for basolateral Na^+ exit in the NHE3 immunopositive cells could be the NBC (Hwang and Lee, 2007, Parks et al., 2007), as it occurs in the proximal tubule of the mammalian kidney (Amlal et al., 2001). Therefore, it might be interesting to find evidence of FW branchial cells expressing both NHE3 and NBC.

Conclusions

This study confirmed that different temperatures influence the number of cells expressing the transporters studied (NKA, NHE3, and V-HAT) in the epithelium of a FW teleost. The highest expression of all three proteins was seen in the lowest temperature, possibly due to decreased activity of the enzymes.

We also observed expected alteration in the gill morphology depending on temperature. The gill lamellae were covered with a cell mass in the lower temperature, whereas they gradually protruded on the surface with the increasing temperature.

A hypothetical model of the ion transporter organization is suggested. Sodium ions can be absorbed into the epithelial cell via an apical Na^+ channel, whereas protons are secreted through H^+-ATPase to maintain the ion balance. The other possible pathway for sodium uptake is via an apical NHE; the driving force for this exchange is provided by protons originating from H_2CO_3 dissociation. Sodium exits into the plasma via either the basolateral Na^+/K^+ ATPase, or Na^+/HCO_3^- co-transporter.

Further research is needed to find out more on the influence of temperature or hypoxia on ion transporters activity and expression level in the gill epithelium.

References

Amlal, H., Chen, Q., Greeley, T., Pavelic, L., Soleimani, M., 2001. Coordinated down-regulation of NBC-1 and NHE-3 in sodium and bicarbonate loading. Kidney International 60: 1824-1836.

Avella, M., Bornancin, M., 1989. A new analysis of ammonia and sodium transport through the gills of the freshwater rainbow trout (*Salmo gairdneri*). J. exp. Biol. 142, 155-175.

Axelrod, H. R., Balon, E., Hoffman, R. C., Rothbard, S., Wohlfarth, G., 1996. The completely illustrated guide to koi for your pond. T.F.H. Publications, Inc., 312 p.

Balon, E. K., 1995. Origin and domestication of the wild carp, Cyprinus carpio: from Roman gourmets to the swimming flowers. Aquaculture 129: 3-48.

Blanco, G., Mercer, R., W., 1998. Isozymes of the Na-K-ATPase: heterogeneity in structure, diversity in function. Am. J. Physiol. Renal. Physiol. 275: 633-650.

Blažka, P., 1958. O biologii karasia obyknobennogo (*Carassius carassius* L. morpha *humilis heckel*). Zoologičeskij žurnál XXXIX, vyp. 9, 1384–1389.

Chang, I. C., Lee, T. H., Yang, C. H., Wei, Y. Y., Chou, F. I., Hwang, P. P., 2001. Morphology and function of gill mitochondria-rich cells in fish acclimated to different environments. Physiol. Biochem. Zool. 74(1): 111-119.

Choe, K. P., O'Brien, S., Evans, D. H., Toop, T., Edwards, S. L., 2004. Immunolocalization of Na^+/K^+-ATPase, carbonic anhydrase II, and vacuolar H^+-ATPase in the gills of freshwater adult lampreys, *Geotria australis*. J. Exp. Zool. 301A: 654-665.

Claiborne, J. B., Edwards, S. L., Morrison-Shetlar, A. I., 2002. Acid-base regulation in fishes: cellular and molecular mechanisms. J. Exp. Zool. 293: 302-319.

Daborn, K., Cozzi, R. R. F., Marshall, W. S., 2001. Dynamics of pavement cell-chloride cell interactions during abrupt salinity change in Fundulus heteroclitus. J. Exp. Biol. 204: 1889-1899.

Dobíhal, R., Blažka, P., 1974. Výzkum přípustných hodnot dlouhodobého deficitu rozpuštěného kyslíku v tocích ve vztahu k rybím pásmům. Reseacrh report.

Evans, D. H., Piermarini, P. M., Choe, K. P., 2005. The multifunctional fish gill: dominant site of gas exchange, osmoregulation, acid-base regulation, and excretion of nitrogenous waste. Physiol. Rev. 85: 97-177.

Galvez, F., Reid, S. D., Hawkins, G., Goss, G. G., 2002. Isolation and characterization of mitochondria-rich cell types from the gill of freshwater rainbow trout. Am. J. Physiol. Regulatory Integrative Comp. Physiol. 282: R658-R668.

Graham, J. B., Aquatic and aerial respiration, in The physiology of fishes. 3rd Ed. Evans, D. H., Claiborne, J. B., 2006. Taylor & Francis Group, LLC. 601 p., Chapter 3.

Hanel, L., 1998. Svět zvířat VIII. Ryby (1). Albatros. 150 p.

Hirata T., Kaneko, T., Ono, T., Nakazato, T., Furukawa, N., Hasegawa, S., Wakabayashi, S., Shigekawa,, M., Chnag, M. H., Romero, M., F., Hirose, S., 2003. Mechanism of acid adaptation of a fish living in a pH 3.5 lake. Am. J. Physiol. Regul. Integr. Comp. Physiol. 284: R1199-R1212.

Hochachka, P. W., Lutz, P. L., 2001. Mechanism, origin, and evolution of anoxia tolerance in animals. Comp. Bioch. Physiol. B130: 435-459.

Hwang, P., Lee, T., 2007. New insights into fish ion regulation and mitochondrion-rich cells. Comp. Bioch. Phys. A, article in press.

Katoh, F., Hyodo, S., Kaneko, T., 2002. Vacuolar-type proton pump in the basolateral plasma membrane energizes ion uptake in branchial mitochondria-rich cells of killifish *Fundulus heteroclitus*, adapted to a low ion environment. J. Exp. Biol. 206: 793-803.

Kratochvilová, H., 2005. Vliv oxidu uhličitého a aklimační teploty na rezistenci karasů proti anoxii. Bachelor thesis. Unpublished.

Lin, H., Pfeiffer, D. C., Vogl, A. W., Pan, J., Randall, D. J., 1994. Immunolocalization of H^+-ATPase in the gill epithelia of rainbow trout. J. exp. Biol. 195, 169–183.

Marshall, W. S., Grosell, M., Ion transport, osmoregulation, and acid-base balance, in The physiology of fishes. 3rd Ed. Evans, D. H., Claiborne, J. B., 2006. Taylor & Francis Group, LLC. 601 p., Chapter 6.

Metz, J. R., van den Burg, E. H., Bonga, S. E. W., Flik, G., 2003. Regulation of branchial Na^+/K^+-ATPase in common carp *Cyprinus carpio* L. acclimated to different temperatures. J. Exp. Biol. 206: 2273-2280.

Moyes, C. D., Schulte, P. M., 2006. Principles of animal physiology. Pearson Education, Inc., 733 p.

Nelson, N., Harvey, W., 1999. Vacuolar and plasma membrane proton-adenosinetriphosphatases. Physiol. Rev. 79: 361-385.

Orlowski, J., Grinstein, S., 1997. Na^+/H^+ exchangers of mammalian cells. J. Biol. Chem. 272: 22373-22376.

Parks, S. K., Tresguerres, M., Goss, G. G., 2007. Interactions between Na^+ channels and Na^+-HCO_3^- cotransporters in the freshwater fish gill MR cell: a model for transepithelial Na^+ uptake. Am. J. Physiol. Cell Physiol. 292: C935-C944.

Perry, S. F., 1997. The chloride cell: structure and function in the gills of freshwater fishes. Annu. Rev. Physiol. 59: 325-47.

Perry, S. F., Gilmour, K. M., 2006. Acid-base balance and CO_2 excretion in fish: unanswered questions and emerging models. Respir. Physiol. Neurobiol. 154: 199-215.

Piermarini, P. M., Evans, D. H., 2001. Immunochemical analysis of the vacuolar proton-ATPase B-subunit in the gills of a euryhaline stingray (*Dasyatis sabina*): effects of salinity and relation to Na^+/K^+-ATPase. J. Exp. Biol. 204: 3251-3259.

Pisam, M., Massa, F., Jammet, C., Prunet, P., 2000. Chronology of the appearance of α, A, and β mitochondria-rich cells in the gill epithelium during ontogenesis of the brown trout (*Salmo trutta*). The Anatomical Record 259: 301-311.

Randall, D., 1982. The control of respiration and circulation in fish during exercise and hypoxia. J. Exp. Biol. 100: 275-288.

Randall, D.J., Burggren, W., French, K., 2002. Eckert Animal physiology. Mechanisms and adaptations. 5th Ed. W.H. Freeman and Company. 736 p.

Randall, D. J., Hung, C. Y., Poon, W. L., 2004. Response of aquatic vertebrates to hypoxia. Fish physiology, toxicology, and water quality. Proceedings of the eighth international symposium, Chongquing, China.

Reichholf, J. H., Steinbach, G., 2002. Zoologická encyklopedie. Ryby. Euromedia Group k. s. 160 p.

SCION CORPORATION 2000. Scion Image for Windows.(downloaded: November, 11th, 2007, http://www.meyerinst.com/html/scion/scion_image_windows.htm).

Scott, G. R., Claiborne, J. B., Edwards, S. L., Schulte, P. M., Wood, C. M., 2005. Gene expression after freshwater transfer in gills and opercular epithelia of killifish: insight into divergent mechanisms of ion transport. J. Exp. Biol. 208: 2719-2729.

Singer, T. D., Tucker, S. J., Marshall, W. S., Higgins, C. F., 1998. A divergent CFTR homologue: highly regulated salt transport in the euryhaline teleost F. heteroclitus. Am. J. Physiol. Cell Physiol. 274: 715-723.

Sollid J., De Angelis, P., Gundersen, K., Nilsson, G. E., 2003. Hypoxia induces adaptive and reversible gross morphological changes in crucian carp gills. J. Exp. Biol. 206: 3667-3673.

Sollid J., Weber, R. E., Nilsson, G. E., 2005. Temperature alters the respiratory surface area of crucian carp *Carassius carassius* and goldfish *Carassius auratus*. J. Exp. Biol. 208: 1109-1116.

StatSoft, Inc., 2001. STATISTICA (data analysis software system), version 7., viz: www.statsoft.com.

Stensløkken, K.-O., Sundin, L., Nilsson, G. E., 1999. Cardiovascular and gill microcirculatory effects of endothelin-1 in atlantic cod: evidence for pillar cell contraction. J. Exp. Biol. 202: 1151-1157.

Sullivan, G. V.,Fryer, J. N., Perry, S. F., 1995. Immunolocalization of proton pumps (H^+-ATPase) in the pavement cells of rainbow trout. J. exp. Biol. 198, 2619–2629.

van den Thillart, G., van Waarde, A., 1985. Teleosts in hypoxia: aspects of anaerobic metabolism. Molecular Physiology 8, 393–409.

Wang, C., Li, S., 2004. Phylogenetic relationships of ornamental (koi) carp, Oujiang color carp and Lon-fin carp revealed by mitochondrial DNA COII gene sequences and RAPD analysis. Aquaculture 231: 83-91.

Wilson, J. M., Laurent, P., Tufts, B. L., Benos, D. J., Donowitz, M., Vogl, A. W., Randall, D. J., 2000. NaCl uptake by branchial epithelium in freshwater teleost fish: an immunological approach to ion-transport protein localization. J. Exp. Biol. 203: 2279-2296.

Yan, J. J., Chou, M. Y., Kaneko, T., Hwang, P. P., 2007. Gene expression of Na^+/H^+ exchanger in zebrafish H^+-ATPase-rich cells during acclimation to low-Na^+ and acidic environments. Am. J. Physiol. Cell Physiol. Article in press.

Zhou, B. S., Wu, R. S. S., Randall, D. J., Lam, P. K. S., Ip, Y. K., Chew, S. F., 2000. Metabolic adjustments in the common carp during prolonged hypoxia. J. Fish Biology 57: 1160-1171.

SUPPLEMENT

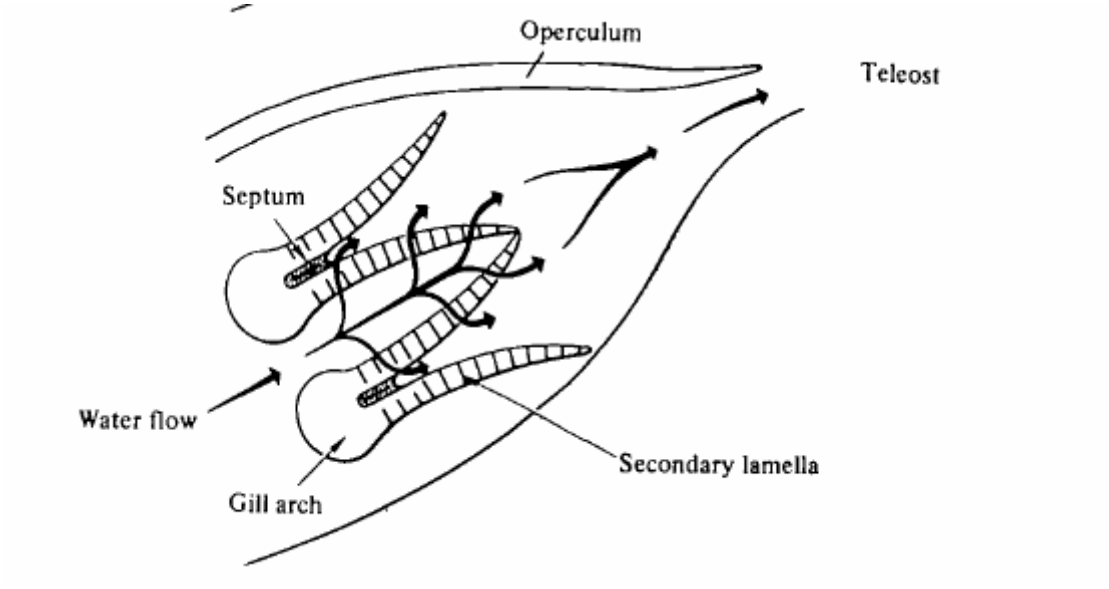

Fig. 1. Dorsal view of the teleost branchial apparatus. Only two gill arches are shown. (from Randall, 1982).

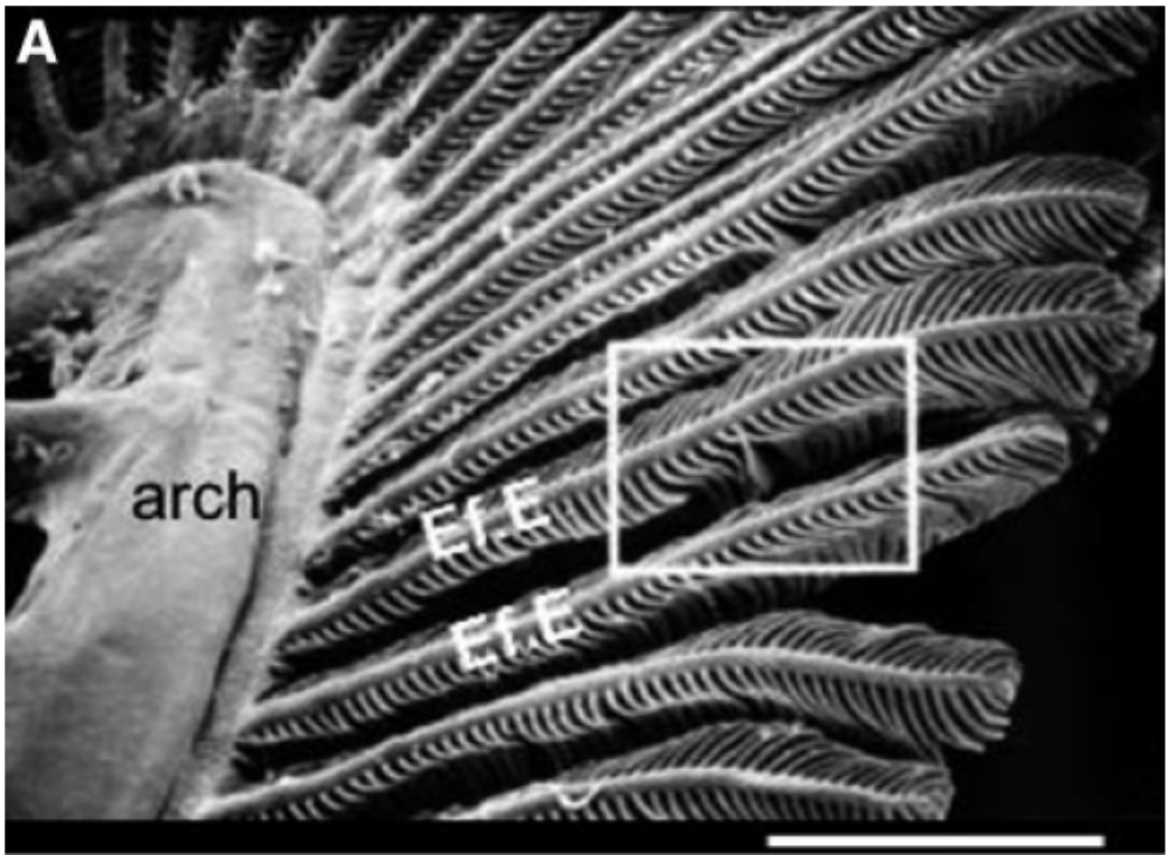

Fig. 2. Scanning electron micrograph of a teleost gill arch with filaments and lamellae. Ef. E – efferent edge. Bar = 100μm. (from Evans et al., 2005).

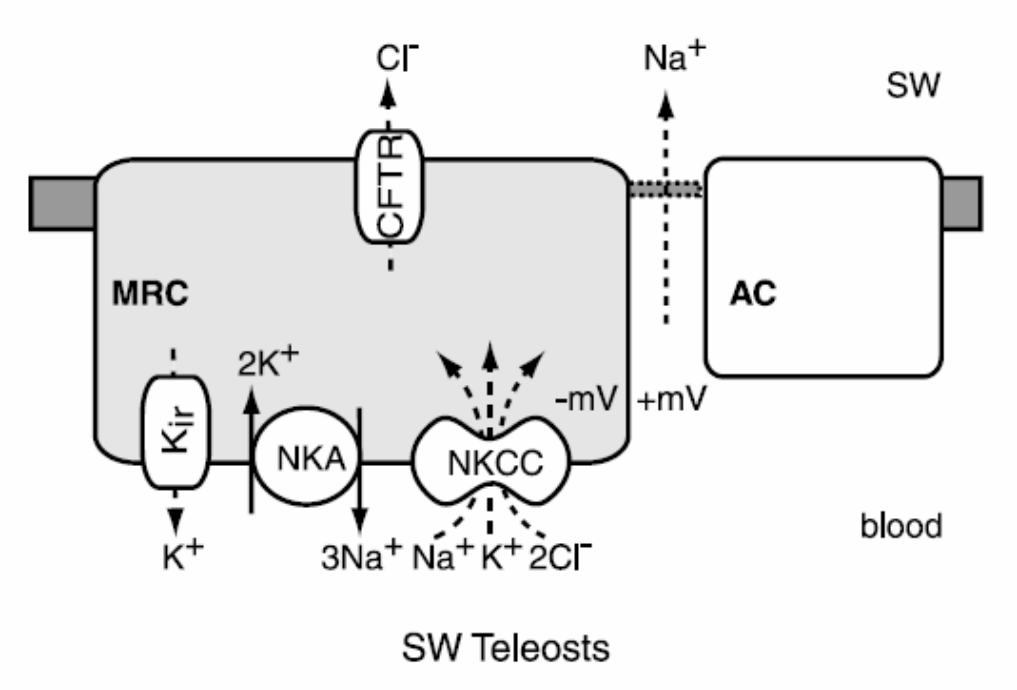

Fig. 3. Model of ion regulatory pathways in seawater branchial epithelium. SW – seawater, MRC – mitochondria rich cell, AC – accessory cell, CFTR – Cl^- channel, K_{ir} – K^+ channel, NKA – Na^+/K^+ ATPase, NKCC – $Na^+/K^+/Cl^-$ co-transporter. (from Evans et al., 2005).

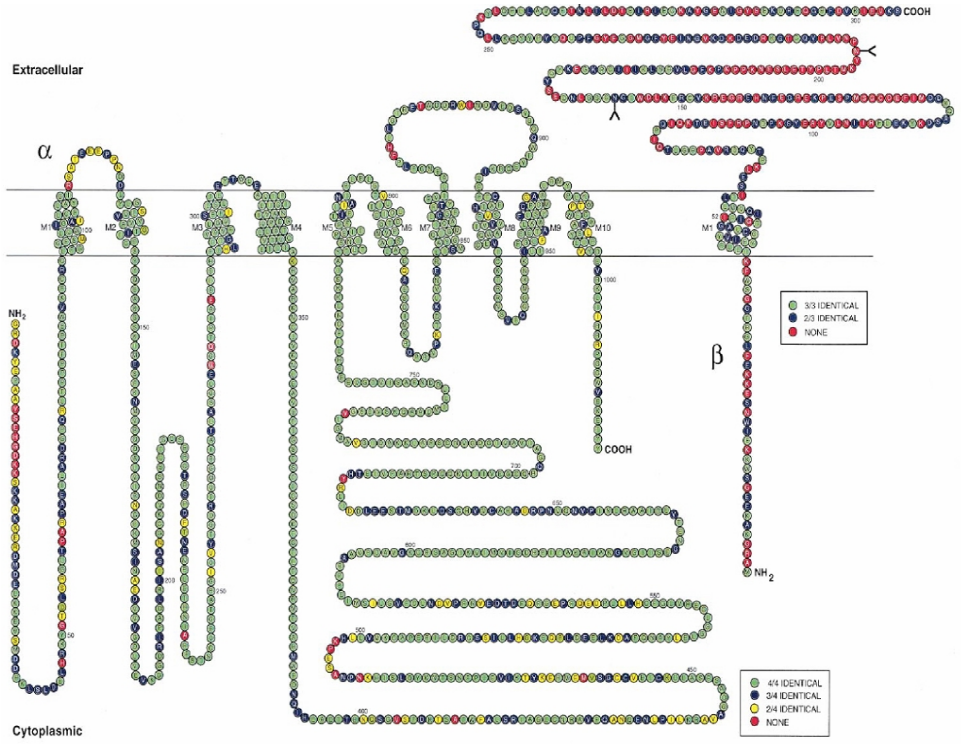

Fig. 4. Na^+/K^+ ATPase from rat – membrane topology of the α- and β- isoforms. (from Blanco and Mercer, 1998).

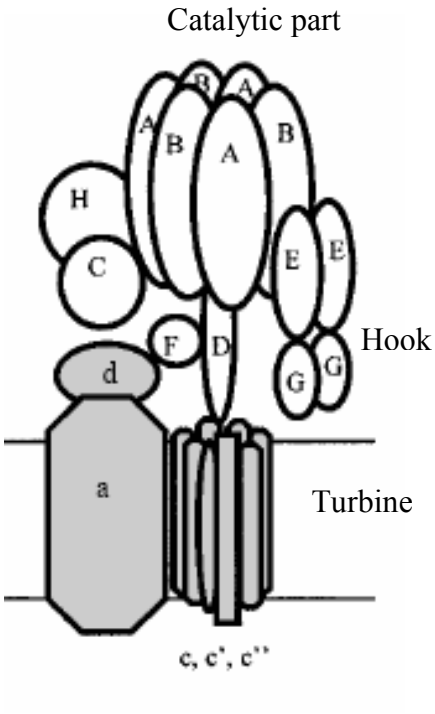

Fig. 5. V-H^+ ATPase of yeast – sub-unit structure and location within the cell membrane. The shaft is represented by 'D' in the scheme. See text for details. (from Nelson and Harvey, 1999).

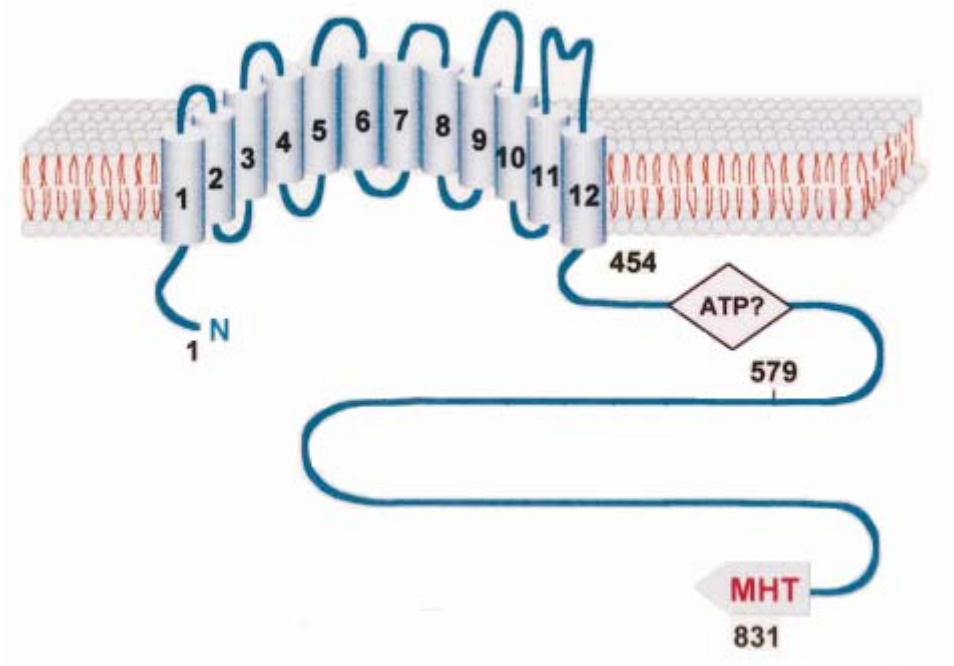

Fig. 6. Na^+/H^+ exchanger of rat. Membrane topology with a large cytoplasmic region at the C-terminus and 12 membrane helixes at the N-terminus. (simplified from Orlowski and Grinstein, 1997.)

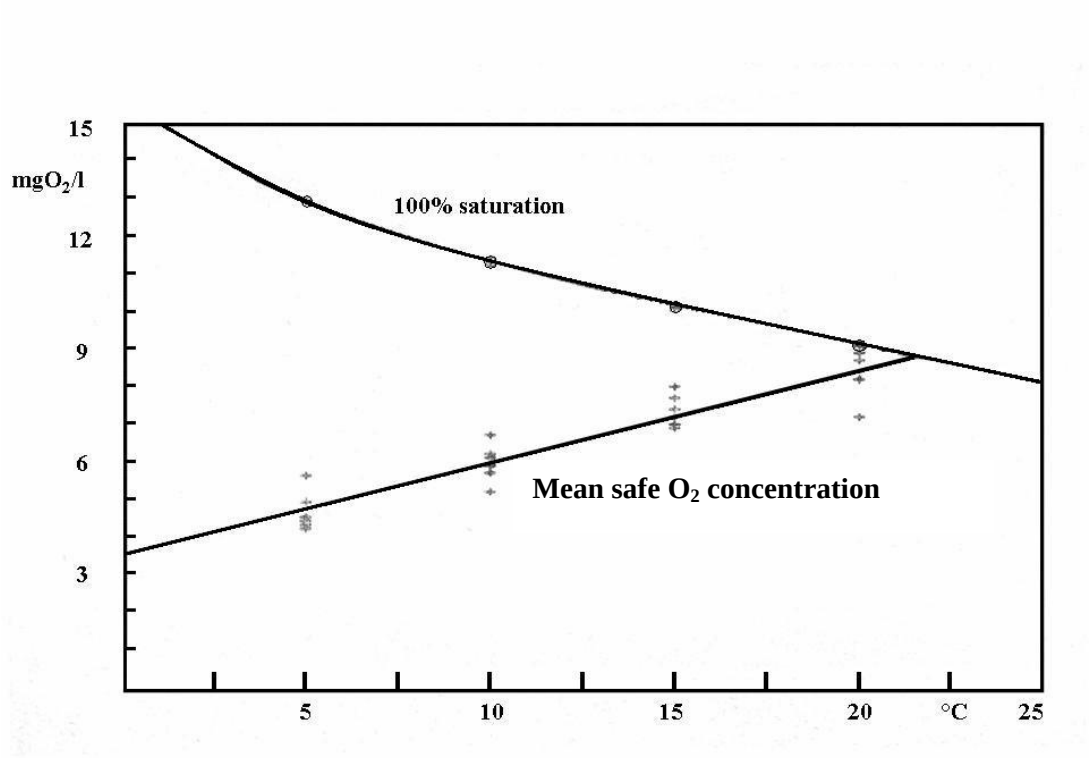

Fig. 7. Safe level of dissolved oxygen for swimming fish increases with temperature, whereas the level of 100% air saturation decreases. At temperatures higher than 22°C, hypoxia is suggested. (modified from Dobíhal and Blažka, 1974).

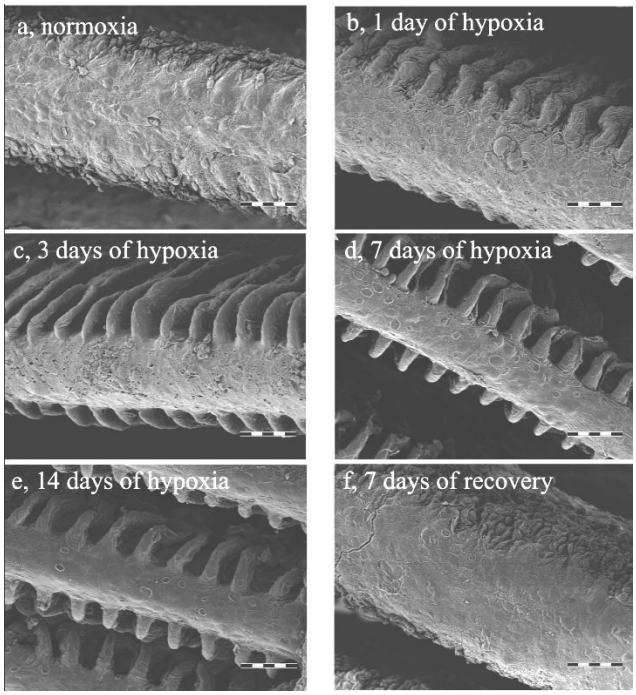

Fig. 8. Scanning electron micrographs of gill arches of Crucian carp in normoxic water, after 1, 3, 7 and 14 days of hypoxia, and after 7 days of recovery. The alteration of gill morphology is shown – the lamellae are covered with a cell mass in normoxic conditions, but protrude on the surface in hypoxia, in order to increase the surface area for a greater gas exchange. Scale bar = 50μm. (from Sollid et al., 2003).

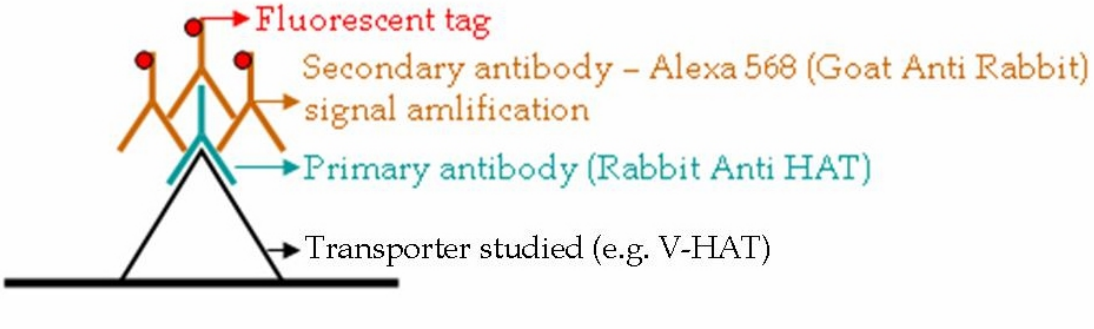

Fig. 9. Simplified scheme of immunohistochemical staining. See text for details.

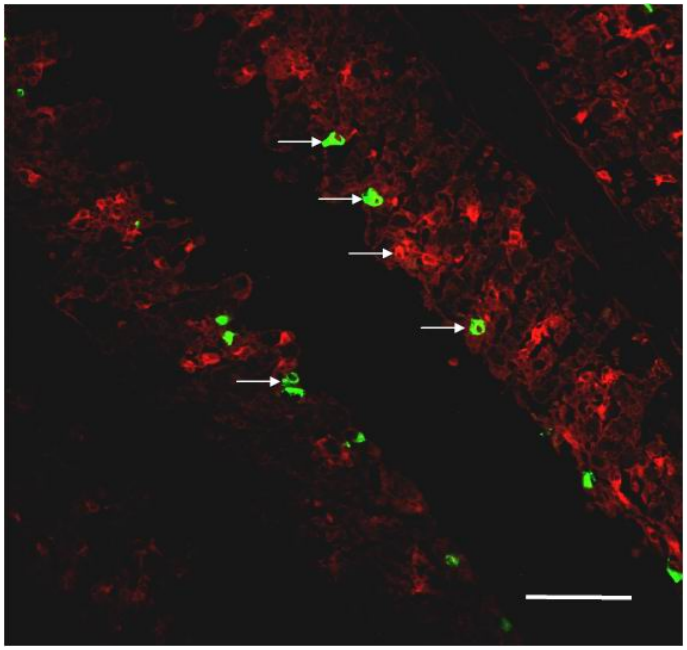

Fig. 10. Confocal merged image of koi carp filament section from the control group with fluorescent staining against NHE3 (red) and NKA (green). Arrows indicate cells with staining throughout the cell body except of the nucleus. Scale bar = 50 μm.

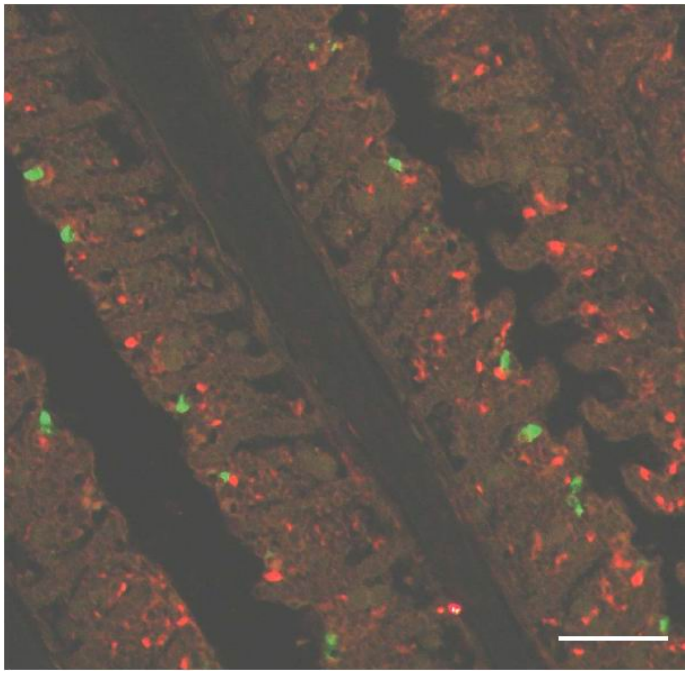

Fig. 11. Fluorescent micrograph of koi section from the control group stained against V-HAT (red) and NKA (green). A lot of cells are immunopositive, NKA and V-HAT do not co-localize to same cells. Scale bar = 50 μm.

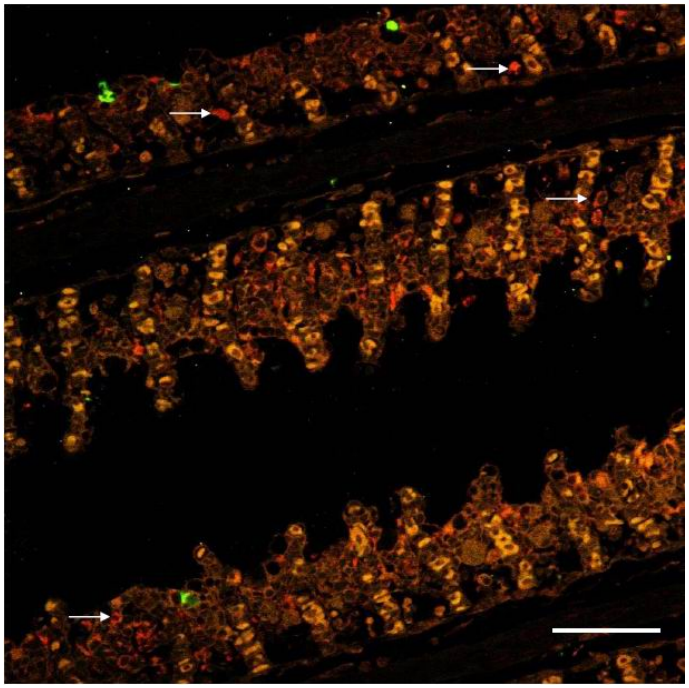

Fig. 12. Confocal micrograph of koi section from the hot group stained against V-HAT (red) and NKA (green). Arrows show some of the V-HAT immunopositive cells, which are much less abundant than in the control group (Fig. 11.). There are also less NKA positive cells. Scale bar = 50 μm.

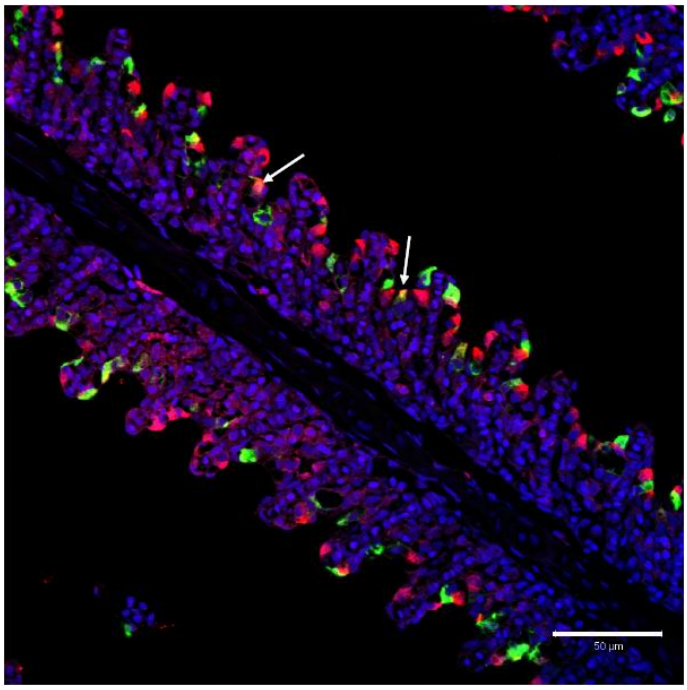

Fig. 13. Confocal merged image of koi section from the control group stained against dNHE3 (red) and NKA (green) and by DAPI (blue – DNA staining, showing cell nuclei). Arrows indicate cells which appear to express both dNHE3 and NKA. Scale bar = 50 μm.

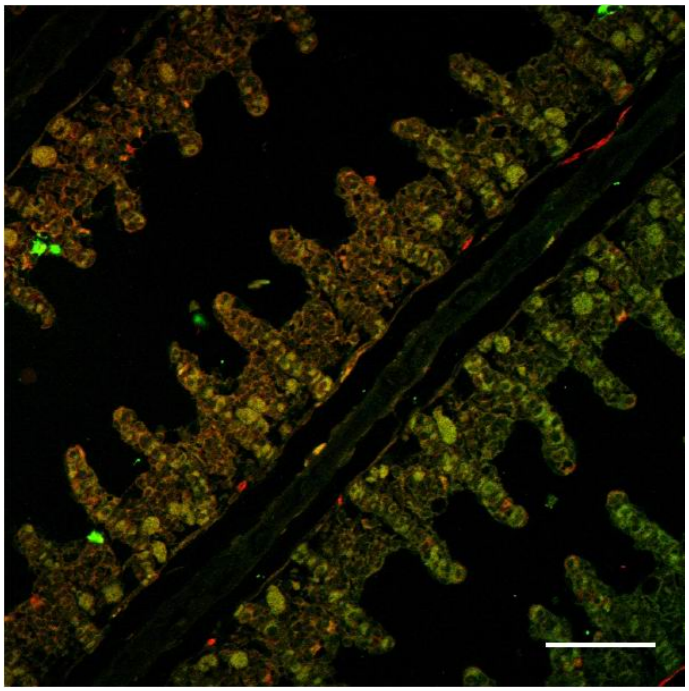

Fig. 14. Confocal merged image of koi section from the hot group stained against dNHE3 (red) and NKA (green), only a few cells are immunopositive. Scale bar = 50 μm.

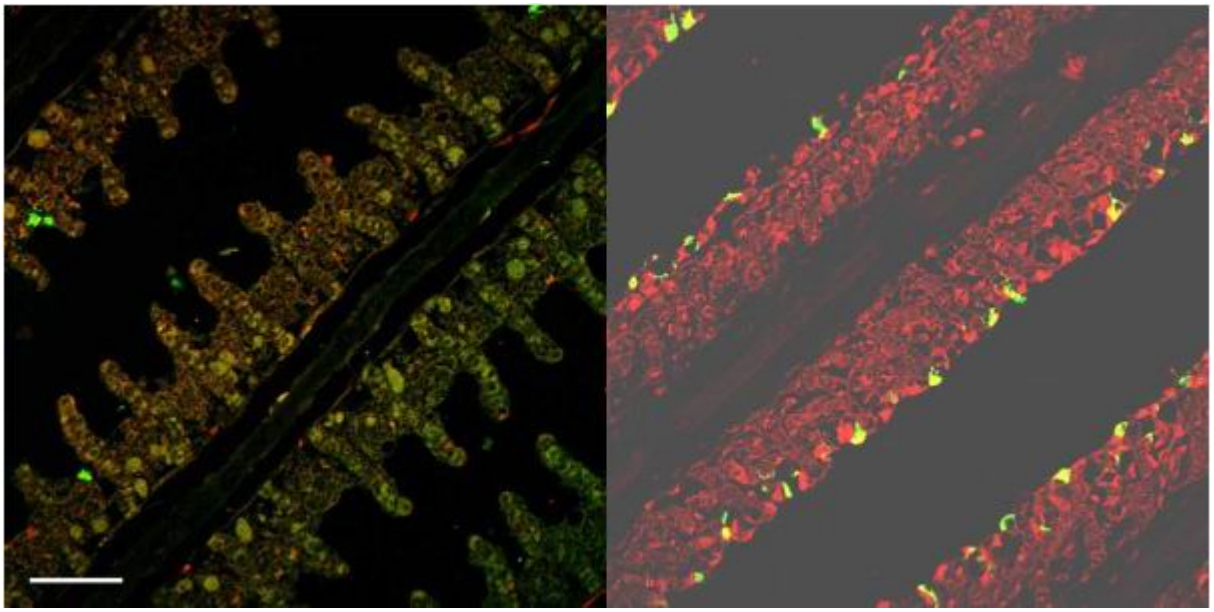

Fig.15. Representative confocal micrographs demonstrating lamellae protruding out of the cell mass at higher temperature (28°C, left), compared to lower temperature (4°C, right). Scale bar, 50 μm.

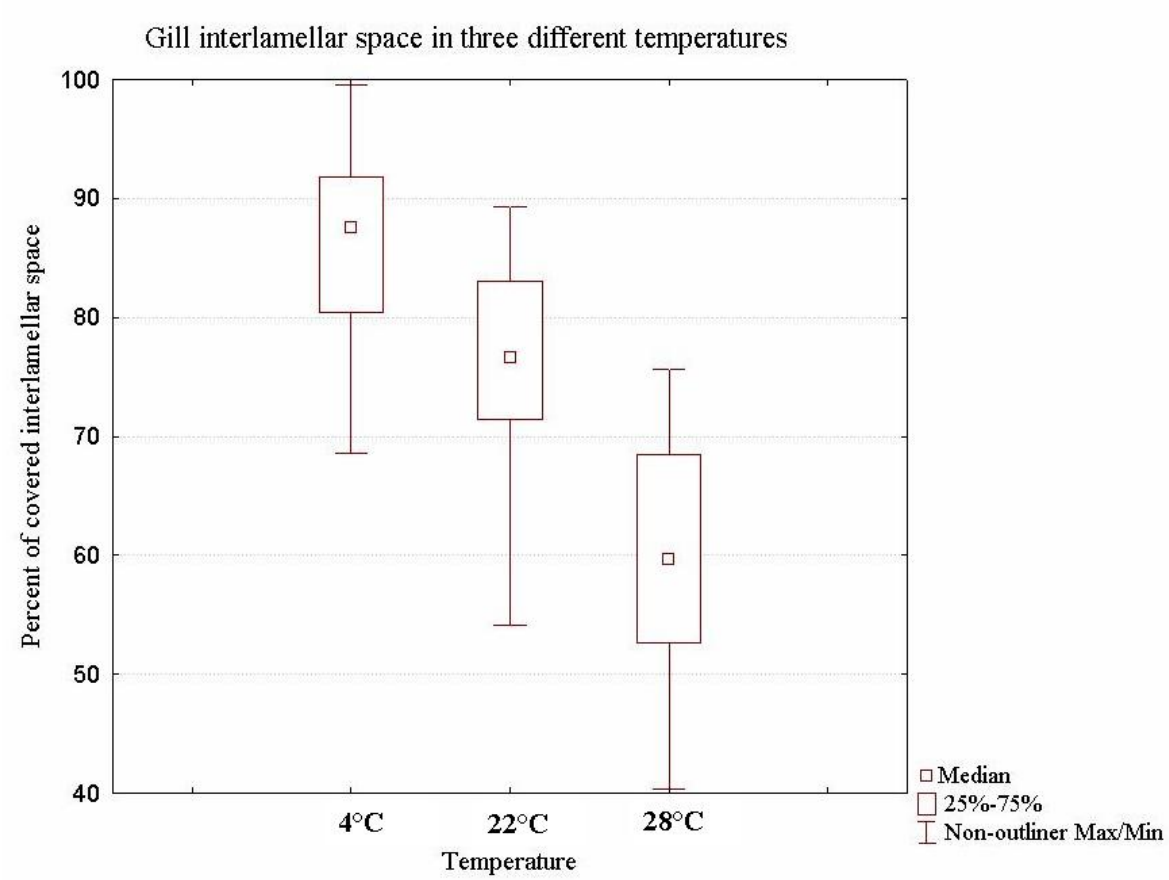

Fig. 16. Box-and-whiskers plot showing the coverage (%) of the interlamellar space in koi branchial epithelium at three different temperatures.

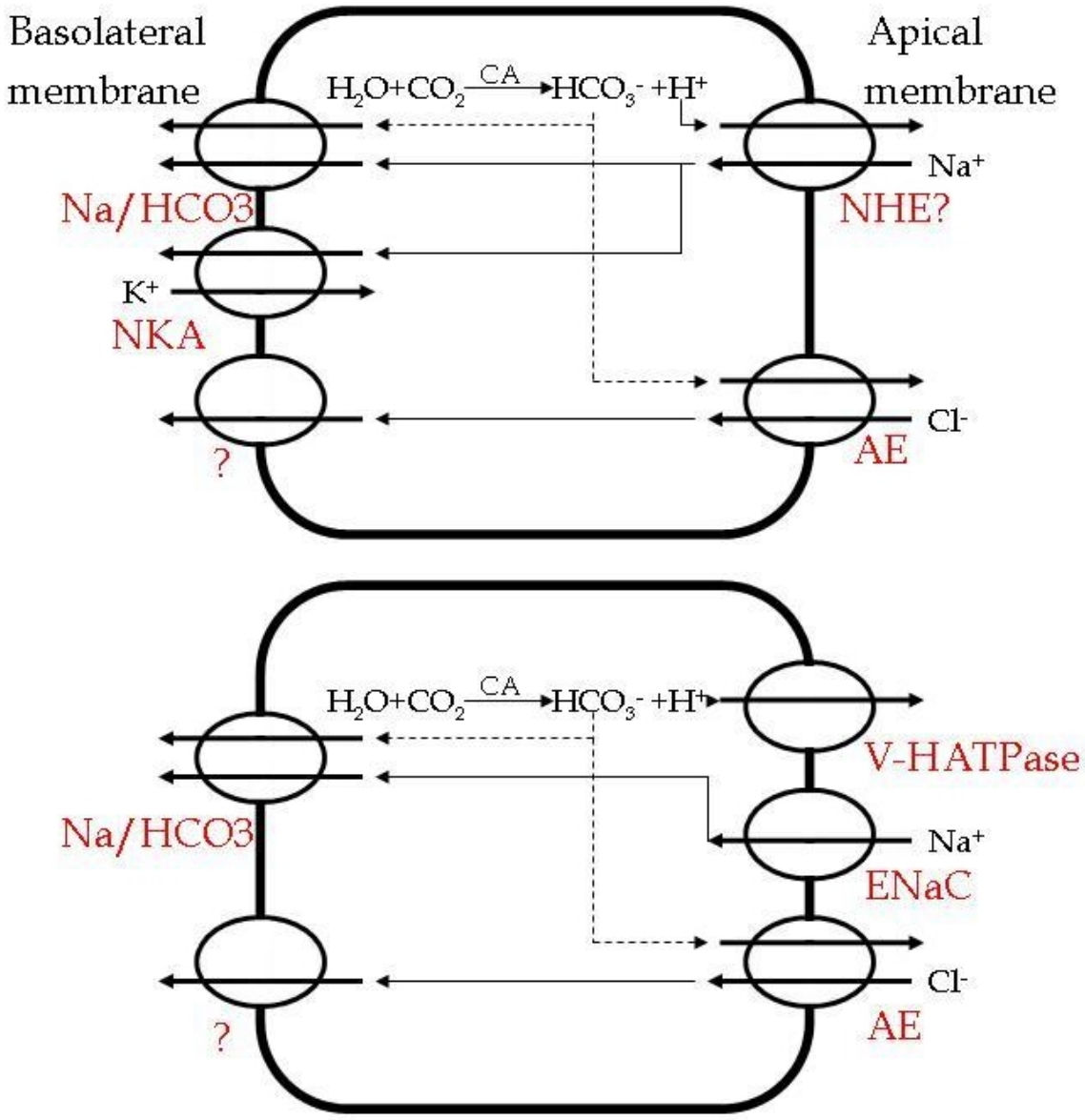

Fig. 17. Proposed model of NaCl uptake in freshwater ionocytes. Na/HCO3 – Na^+/HCO_3^- co-transporter, NKA – Na^+/K^+ ATPase, NHE – Na^+/H^+ exchanger, AE – anion exchanger, V-HATPase – V-type H^+ ATPase, ENaC – epithelial Na^+ channel, CA – carbon anhydrase, '?' represents the possible Cl^- basolateral exit via CFTR-like anion channel. See text for details.